

din, C. P. Ryan, *Theory of Weak Interactions* (Interscience, New York, 1969).

¹⁰The region $\theta_e \geq 3\pi/4$ where our detection efficiency

is low is excluded. This removes 1.5% of the events from each sample.

¹¹S. L. Glashow, *Phys. Rev. Lett.* **14**, 35 (1965).

Charged-Particle Multiplicity Distribution from 200-GeV pp Interactions*

G. Charlton, Y. Cho, M. Derrick, R. Engelmann, T. Fields, L. Hyman, K. Jaeger, U. Mehtani, B. Musgrave, Y. Oren,† D. Rhines, P. Schreiner, and H. Yuta

Argonne National Laboratory, Argonne, Illinois 60439

and

L. Voyvodic, R. Walker, and J. Whitmore

National Accelerator Laboratory, Batavia, Illinois 60510

and

H. B. Crawley

Iowa State University, Ames, Iowa 50010

and

Z. Ming Ma

Michigan State University, East Lansing, Michigan 48823

and

R. G. Glasser‡

University of Maryland, College Park, Maryland 20742

(Received 21 July 1972)

From 2728 events of 205-GeV pp interactions found in 15 000 pictures taken with the 30-in. hydrogen bubble chamber at the National Accelerator Laboratory, a total cross section of 39.5 ± 1.1 mb was measured. The mean charged-particle multiplicity for inelastic pp collisions was measured to be 7.65 ± 0.17 . The prong distribution from 2 to 22 prongs is broader than a Poisson distribution and has a width parameter $f_2^- = \langle n_-(n_- - 1) \rangle - \langle n_- \rangle^2 = 0.95 \pm 0.21$.

In this Letter we present data on pp interactions observed in the 30-in. hydrogen bubble chamber at the National Accelerator Laboratory. Although many aspects of this exposure are still being studied, we present the results on the charged-prong multiplicity distributions because of the current interest in such properties of high-energy interactions.

The proton beam from the separated-function synchrotron operating at 205 GeV was extracted and passed through a series of collimators and magnetic lenses to reduce the intensity from $\sim 10^9$ to a few protons per pulse. After momentum analysis and shaping, the beam entered the 30-in. hydrogen bubble chamber. The chamber was operated at a magnetic field of 27 kG and four views were photographed on 70-mm film.

The total of about 15 000 good pictures was divided into two equal samples which were indepen-

dently analyzed by two groups of the authors. The film was scanned by the authors using all four views on a projection of 90% life size. The fiducial volume in space was about 40 cm along the beam direction. In the scan, the following were recorded: (1) the number of charged prongs, (2) associated V^0 decays and γ conversions, (3) charged decays of prongs from the main vertex, (4) obvious Dalitz pairs, recognized by the spiralization or bubble density and curvature of an electron track, (5) associated neutron stars, and (6) any secondary interactions of the particles from the primary vertex. The frames used in this experiment were quite free of background tracks, and the optical quality of the track images is outstanding in this chamber, so that no trouble was experienced in recognizing the events.

For each acceptable frame, a beam count was made. An average of 3.5 beam tracks entered

the chamber for each acceptable picture. In general, nonbeam tracks were easily recognizable since the beam in the chamber was tightly collimated.

About one quarter of the film was scanned a second time. A comparison of the results showed that for the frames that were used for this experiment, the average scanning efficiency was $(99 \pm 1)\%$ except for the two-prong topology, where it was estimated to be $(96 \pm 3)\%$. Although the second scan showed that a complete rescan of the pictures was not necessary, it also revealed some discrepancies between the two scans in counting the number of prongs associated with the events. These discrepancies were due mainly to the high multiplicity and forward collimation of the secondaries from the events. To overcome this problem, all 2728 events were re-examined using a table on which the pictures were projected approximately 6 times life size. With this large magnification, there were only 38 events for which the prong count could not be resolved, usually because of a close secondary interaction. In addition, a number of hitherto unseen secondary interactions, V^0 decays, and γ conversions were found. A comparison of the results of the two groups of authors was made after this editing procedure. No significant differences were found, so the data were combined.

Several small corrections were applied to the raw numbers of events listed in Table I. The correction for secondary interactions so close to

the primary vertex that the primary and secondary vertices could not be distinguished was found to be negligible. Obvious Dalitz pairs were excluded from the prong count in the scanning. The correction for Dalitz pairs that could not be recognized on the scanning table was made by using the observed external γ conversions. These are estimated to be ~ 3.8 times more probable than internal conversions.¹ A second small correction was made for external pairs and V^0 decays occurring so close to the main vertex that the V^0 decay tracks could not be distinguished from tracks from the main vertex. The 38 events whose prong count was odd or could not be resolved were assigned to the best estimate of the prong count, and the errors associated with that and neighboring bins were suitably increased.

The two-prong events require an additional correction for the usual loss of very peripheral events, because the proton stub was too short to be seen easily. This correction was measured from the t distribution obtained after measuring a sample of the two-prong events on the automatic measuring device POLLY and reconstructing

TABLE I. Topological cross sections in 205-GeV pp interactions.

Number of prongs	Events found	Corrected number	Cross section (mb)
2 Total	608	745 ± 68	10.29 ± 0.92
Elastic		493 ± 22	$(6.8 \pm 0.3)^a$
Inelastic		252 ± 63	3.49 ± 0.87
4	398	402 ± 20	5.55 ± 0.28
6	502	502 ± 23	6.94 ± 0.31
8	419	419 ± 21	5.78 ± 0.28
10	323	319 ± 18	4.41 ± 0.25
12	250	248 ± 16	3.43 ± 0.22
14	125	123 ± 12	1.70 ± 0.16
16	64	63 ± 8	0.87 ± 0.11
18	22	22 ± 5	0.30 ± 0.07
20	13	13 ± 4	0.17 ± 0.05
22	4	4 ± 2	0.05 ± 0.03
Total			39.5 ± 1.1
Inelastic			32.7 ± 1.2

^aInput numbers, see text.

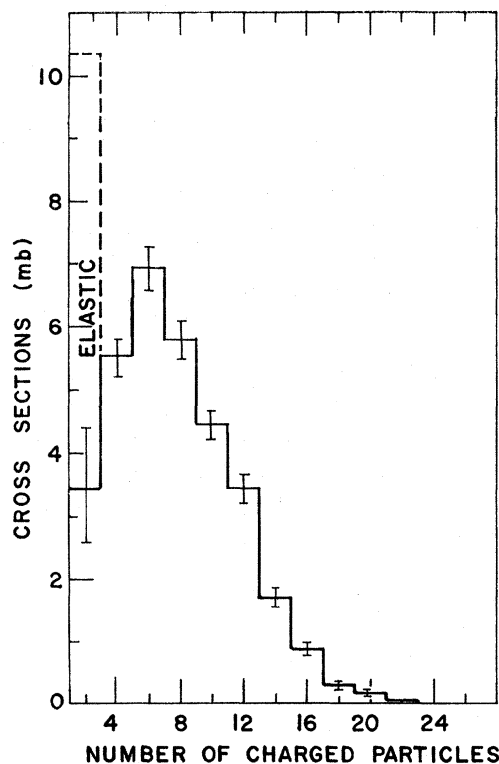


FIG. 1. Partial cross sections for events with 2 through 22 prongs. The dashed histogram shows the contribution of elastic scattering to the two-prong events.

TABLE II. Multiplicity parameters.

	$\langle n \rangle$	$\langle n(n-1) \rangle$	$f_2 = \langle n(n-1) \rangle - \langle n \rangle^2$
Both charges	7.65 ± 0.17	65.9 ± 2.2	7.44 ± 0.72
Negative charge	2.82 ± 0.08	8.92 ± 0.35	0.95 ± 0.21

them using the program TVGP. The correction was $(17 \pm 7)\%$ using the fitted t dependence of $\exp[(9.3 \pm 1.4)t]$.² These events were further corrected for the random scanning loss of 4%.

The number of inelastic two-prong events was estimated using an elastic cross section of 6.8 ± 0.3 mb, which was obtained using the known t dependence of high-energy pp scattering² and the optical point calculated from the total cross section.³

The result of these corrections and their effect on the error is shown in Table I. It is clear that except for the special case of the two-prong topology, the corrections are small compared to the statistical error on the number of events in each multiplicity channel.

The numbers of events were converted to cross sections using the track count and a hydrogen density of 0.0625 ± 0.0006 g cm⁻³ and assuming a beam purity of 100%.⁴ An examination of the angles of reconstructed beam tracks and the beam tracks of the two- and four-prong events showed a maximum systematic error of 2% in the cross section arising from the possible inclusion of events originating from off-angle tracks. The total cross section for the events observed in this experiment is 37.7 ± 0.8 mb which becomes 39.5 ± 1.1 mb after applying the corrections discussed above.

Figure 1 displays the data of Table I. The distribution is relatively broader than observed at lower energies, and broader than would be given by a Poisson distribution of the same mean. The mean number of charged particles per inelastic pp collision at 205 GeV is $\langle n \rangle = 7.65 \pm 0.17$. This may be contrasted with the value of 4.6 ± 0.1 at 28.5 GeV.⁵ The mean number of negatively charged particles is $\langle n_- \rangle = 2.82 \pm 0.08$. The distribution of Fig. 1 may be characterized by the parameters given in Table II.

Our mean multiplicity is not in agreement with the results of the cosmic-ray experiment at Echo Lake⁶ as can be seen in Fig. 2(a) which shows the energy dependence of $\langle n_- \rangle$. The discrepancy may arise from the restricted angular coverage of the spectrometer used in the Echo Lake experi-

ment. Assuming there are no systematic differences between the remaining experiments, then the results shown in Fig. 2(a) are not fitted well by a single log term for the energy variation of $\langle n_- \rangle$ between 13 and 200 GeV. It is clear that accurate knowledge of the momentum dependence requires systematic studies in the several-hundred-GeV region. Our value for f_2^- as seen in Fig. 2(b) shows unambiguously that the multiplicity distribution changes from being narrower than a Poisson at ~ 20 GeV to wider at 200 GeV.

Comparing our cross-section data with previous experiments, one notes that the cross sections for 10 through 22 prongs are still rising at

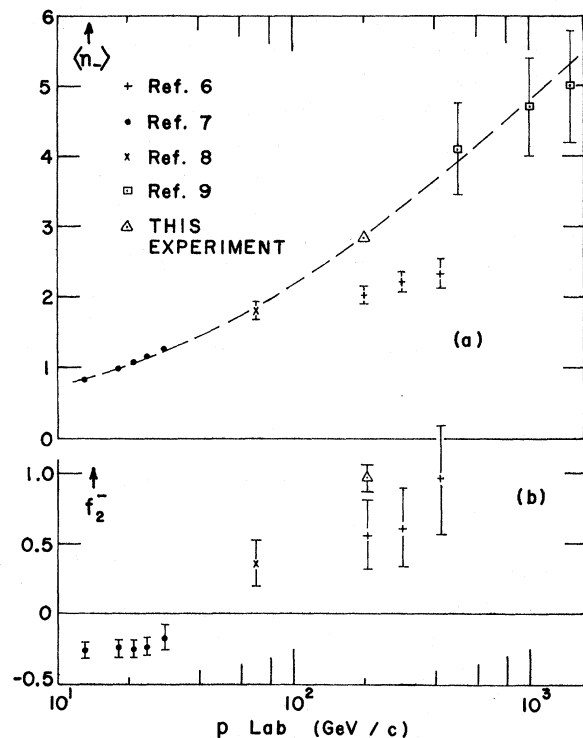


FIG. 2. (a) Mean number of negative particles per inelastic pp collision $\langle n_- \rangle$ as a function of laboratory momentum p . The dashed line is to guide the eye and represents the function $\langle n_- \rangle = 0.19 \pm 0.003 \ln p + 0.095 (\ln p)^2$. (b) Width parameter of the distribution of negative prong numbers $f_2^- = \langle n_- (n_- - 1) \rangle - \langle n_- \rangle^2$ as a function of laboratory momentum. f_2^- changes sign between the low-energy data and the high-energy data.

200 GeV as the momentum increases, whereas the 6- and 8-prong cross sections are almost constant between 70 and 200 GeV. Between 28.5 and 205 GeV, the four-prong cross section falls slowly ($\sim p^{-0.4}$), perhaps indicating the presence of a diffractive component in the four-prong topology.

This experiment was made possible only by the dedicated work of the staff of the National Accelerator Laboratory and the people from Argonne National Laboratory who were responsible for transferring the chamber. To all of them we express our appreciation.

*Work supported by the U. S. Atomic Energy Commission.

†On leave from Tel-Aviv University, Tel-Aviv, Israel.

‡Presently on leave at Argonne National Laboratory.

¹The total corrected number of Dalitz pairs was in reasonable agreement with estimates made of the mean number of π^0 's, which in turn was estimated from the number of charged particles. See Ref. 9.

²This may be compared with the elastic t dependence of e^{11t} measured by G. Barbiellini *et al.*, Phys. Lett. **39B**, 663 (1972).

³The total cross section of 38.2 ± 0.2 mb was taken

from the compilation of V. Barger and R. J. N. Phillips, Nucl. Phys. **B40**, 205 (1972). The elastic cross section agrees with 6.8 ± 0.6 mb measured at the intersecting storage rings by M. Holder *et al.*, Phys. Lett. **35B**, 361 (1971).

⁴From the design of the beam transport system, one would not expect any substantial hadron or lepton contamination. However, the time structure and instrumentation of the beam did not allow measurement of a possible light-particle contamination. One should then consider the cross sections given in this paper as lower limits.

⁵W. H. Sims *et al.*, Nucl. Phys. **B41**, 317 (1972).

⁶L. W. Jones *et al.*, Nucl. Phys. **B43**, 477 (1972).

⁷E. L. Berger, B. Y. Oh, and G. A. Smith, ANL Report No. ANL-HEP 7209, 1972 (to be published).

⁸Soviet-French Collaboration, Mirabelle experiment at 69 GeV/c, February 1972 (unpublished).

⁹The data shown in Fig. 2(a) are for $\langle n_{\pi^0} \rangle$ and come from the work of G. Neuhofer *et al.* [Phys. Lett. **37B**, 438 (1971), and Phys. Lett. **38B**, 51 (1972)] who measured the γ rays from pp collisions in the CERN intersecting storage rings. G. R. Charlton and G. H. Thomas [ANL Report No. ANL-HEP 7217, 1972 (to be published)] show that the results are consistent with $\langle n_{\pi^0} \rangle = \frac{1}{2}[\langle n_{\pi^+} \rangle + \langle n_{\pi^-} \rangle]$. If this is combined with the π^+ and π^- measurements from the intersecting storage rings [L. G. Ratner *et al.*, Phys. Rev. Lett. **27**, 68 (1971); A. Bertin *et al.*, Phys. Lett. **38B**, 260 (1972)], which show $\langle n_{\pi^+} \rangle \simeq \langle n_{\pi^-} \rangle$, one concludes $\langle n_{\pi^-} \rangle \simeq \langle n_{\pi^0} \rangle$.

Parity Violation in Neutron-Capture γ Rays*

J. L. Alberi and Richard Wilson

Department of Physics, Harvard University, Cambridge, Massachusetts 02138

and

I. G. Schröder

Institute for Basic Standards, National Bureau of Standards, Washington, D. C. 20234

(Received 5 July 1972)

We have measured the circular polarization of γ rays from thermal neutron capture in ^{113}Cd and find a $P_\gamma = (6.0 \pm 1.5) \times 10^{-4}$ for the combined 8.51- and 9.04-MeV transitions. This value was measured using a transmission Compton polarimeter and pulse-counting technique. The value confirms the existence of parity-nonconserving terms in the internucleon force.

Several theories of weak interactions suggest that parity-nonconserving effects may be seen in the internucleon force.¹ One such effect is the circular polarization of neutron-capture γ rays. The present experiment measures this effect in the reaction $^{113}\text{Cd}(n, \gamma)^{114}\text{Cd}$. Thermal-neutron capture on ^{113}Cd populates a high-energy capture state that is 9.04 MeV above the ground state and has angular momentum and parity $J^\pi = 1^+$. This

excited state decays via a highly complicated series of γ -ray de-excitations.² The transition (9.04 MeV) direct to the ground state ($J^\pi = 0^+$) and the transition (8.51 MeV) to the first-excited state ($J^\pi = 2^+$) are the γ rays expected to exhibit parity-nonconserving effects. In both of these electromagnetic transitions, the predominant parity-allowed transition is magnetic dipole ($M1$), while any parity-nonconserving admixture to the